NASA TECHNICAL NOTE

NASA TN D-2088

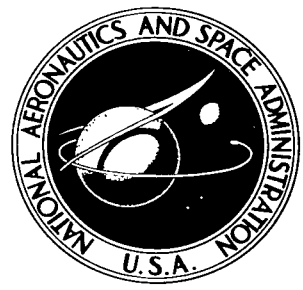

NASA TN D-2088

CAVITATION AND EFFECTIVE LIQUID TENSION OF NITROGEN IN A TUNNEL VENTURI

by Robert S. Ruggeri and Thomas F. Gelder

Lewis Research Center
Cleveland, Ohio

NATIONAL AERONAUTICS AND SPACE ADMINISTRATION • WASHINGTON, D. C. • FEBRUARY 1964

CAVITATION AND EFFECTIVE LIQUID TENSION OF NITROGEN IN A TUNNEL VENTURI

By Robert S. Ruggeri and Thomas F. Gelder

Lewis Research Center
Cleveland, Ohio

NATIONAL AERONAUTICS AND SPACE ADMINISTRATION

For sale by the Office of Technical Services, Department of Commerce,
Washington, D.C. 20230 -- Price $1.00

CAVITATION AND EFFECTIVE LIQUID TENSION

OF NITROGEN IN A TUNNEL VENTURI

SUMMARY

Cavitation of liquid nitrogen was induced on the walls of a Venturi having a 1.377-inch throat diameter in a closed-return hydrodynamic tunnel. Just prior to incipient cavitation, the minimum local wall pressure was significantly less than the vapor pressure corresponding to the stream liquid temperature; this pressure difference is called effective liquid tension. Effective tensions ranged from 8 to 60 feet of nitrogen head for approach velocities from 17 to 55 feet per second, respectively. Temperatures and pressures measured within regions of well-developed cavitation were in thermodynamic equilibrium but were less than the temperature and the saturation vapor pressure of the approaching stream. Measured temperature depressions were as high as 3° F and corresponded to a head depression of 9 feet of liquid nitrogen (at the temperatures studied). These depressions increased with both stream velocity and extent of cavitation.

Compared with previous cavitation tests of room-temperature water in the same Venturi, nitrogen sustained nearly twice the effective tension and exhibited temperature depressions at least one order of magnitude greater.

INTRODUCTION

Cavitation may be described as the formation and subsequent collapse of vapor cavities in a flowing liquid brought about by pressure changes resulting from changes in flow velocity. Cavitation is undesirable because it often results in mechanical damage, noise, and degradation of the flow pattern, which reduces component performance. Experimental studies have shown that water can flow cavitation-free through local regions in which the pressures are considerably lower than the saturation vapor pressure corresponding to the liquid temperature (refs. 1 to 4). In these regions, the liquid is superheated and in a thermodynamically metastable state. The maximum decrement of local pressure relative to vapor pressure occurring at, or just prior to, incipient cavitation is called herein the effective liquid tension. This effective tension can be considered as a pressure difference tending to rupture, or cavitate, the liquid. Effective liquid tension is not the same as the tensile strength of liquids as generally defined in the literature; the latter definition is reserved for pressure decrements relative to an absolute pressure of zero. There is also evidence that, within a cavitated region, the local pressure can be less than the vapor pressure corresponding to the liquid temperature of the approaching stream

(refs. 5 and 6). Such effects are usually attributed to evaporative cooling of the neighboring liquid, which in turn is dependent on the amount of vapor formed during cavitation. These thermodynamic effects are believed to be significant factors affecting cavitating pump performance with liquids of different thermodynamic properties (refs. 6 to 9). As indicated in references 8 and 9, successful prediction of cavitation characteristics of various liquids in hydraulic equipment requires a more basic understanding of such things as nucleation times of metastable (superheated) liquids, rates of cavity formation and vaporization, and temperature and pressure effects within the cavitated region caused by the phase change.

The purposes of this investigation were to study in a flowing system the occurrence and magnitude of effective liquid tension in nitrogen at or near cavitation inception and to determine experimentally temperatures and pressures within cavitated regions. Comparisons were made with measurements taken in water with the identical Venturi. The study was conducted at the NASA Lewis Research Center as part of a general program of cavitation research. The nitrogen cavitation was induced on the walls of a transparent Venturi test section (throat diam., 1.377 in.) in a closed-return tunnel submerged in a liquid-nitrogen bath. The flow velocity in the Venturi approach section was varied from 17 to 55 feet per second, and the resulting tunnel liquid temperatures were between about 140° and 144° R.

APPARATUS

The facility used in the present study is a small closed-return hydrodynamic tunnel designed to handle cryogenic as well as ordinary liquids. For operation with liquid nitrogen, the entire tunnel was submerged in a liquid-nitrogen bath that acted as insulation and as a heat sink for removing the heat imparted to the tunnel liquid by the pump. A schematic drawing and a photograph of the complete facility showing the tunnel-bath arrangement are shown in figures 1(a) and (b), respectively. The tunnel is designed to accommodate 12-inch-long test sections having maximum inlet diameters of 1.743 inches. It is fabricated of aluminum to provide good heat transfer between the tunnel and the bath liquids and has a total liquid capacity of about 10 U.S. gallons. The variable-speed pump-drive system is capable of providing operational flow velocities from about 17 to 85 feet per second at the working-section inlet. The centrifugal pump is a commercially available unit designed to handle cryogenic liquids. Except for minor differences discussed herein, the tunnel portion of the facility is identical to that described in detail in reference 1.

The bath surrounding the tunnel (fig. 1) is fabricated from 304 stainless steel. It is of rigid construction (no flexible joints or bellows) and is insulated with 1/2-inch-thick composition corkboard bonded directly to the metal. Two 8-inch-diameter side windows and one 4-inch-diameter top window are provided for viewing, lighting, and photographing cavitation. The windows, made from 2-inch-thick Lucite, are installed in 304-stainless-steel mounting frames and incorporate ring-type seals of pure lead. Design details are presented in figure 1(c). To allow for dimensional changes of the window with respect to its mounting, each window is provided with a thin-walled (0.005 in.) inflatable

stainless-steel inner tube that, when pressurized (with helium gas from 300 to 1000 lb/sq in. gage), continually forces the window against the primary seal. The window is maintained condensation-free by air jets directed against the outside surface.

Except at the pump end, the tunnel and the bath are supported by adjustable sliding pads to allow for dimensional changes during cooldown. The design pressure range for the bath is 0 to 30 pounds per square inch absolute, and 0.010-inch-thick plastic (polyethylene terephthalate) gaskets were used as seals throughout. The total liquid capacity of the facility is about 70 U.S. gallons.

In addition to measurements in the working section, static pressures were measured in the tunnel expansion chamber, across the contraction nozzle (for flow-velocity determinations), at the pump inlet and outlet flanges, and in the bath ullage space. The liquid levels in the bath and in the tunnel expansion chamber were measured by means of capacitance-type sensors. The sensor in the bath was also used to control bath liquid level automatically. The bath includes a standoff with seals at room temperature to pass the necessary electrical and thermocouple leads. Pressure lines from the tunnel and the test section were passed through multiple-tube gland-type fittings mounted in the bath wall.

A schematic drawing of the valving system and associated facility equipment is shown in figure 2. The equipment consists of a 450-gallon supply Dewar, a vacuum-jacketed fill and drain line, gas pressurization systems (nitrogen and helium), appropriate valving, controls, and safety devices.

Working Sections and Instrumentation

Liquid-nitrogen cavitation studies were made with a Venturi section of transparent acrylic plastic, the same section as used for the water cavitation studies reported in reference 1. As shown in figure 3(a), the Venturi contains a slightly modified quarter round (nominal radius, 0.183 in.), which provides transition from a 1.743-inch approach diameter to a 1.377-inch throat diameter. The 0.75-inch-long throat is followed by a conical diffuser. The actual contour of the modified quarter-round region is presented in figure 3(b). The contour of an enlarged (4.61 scale) aerodynamic Venturi model used for pressure-distribution studies in a wind tunnel is also included.

The 10 static-pressure taps, located as shown in figure 3, are identical to those described in detail in reference 1. For the present study, seven copper-constantan wall thermocouples were installed in the Venturi: three to measure inner- and outer-wall temperature, and four to measure temperatures within the cavitated region. These latter thermocouples were installed in existing pressure taps, as required, with the junctions flush with the Venturi inner wall. The method of installation and thermocouple locations are presented in figure 3(a). Absolute values of tunnel liquid temperature were measured by means of a calibrated platinum resistance thermometer mounted on the tunnel centerline $4\frac{1}{2}$ inches upstream from the contraction nozzle (fig. 1(a)). The temperature measured by the resistance thermometer (to $\pm 0.05^{\circ}$ F) was used for the stream temperature (and

vapor pressure) in the Venturi approach section. (Further discussion is presented in the section Determination of Effective Liquid Tension.) The calibrated thermocouple circuit used to determine temperatures within the Venturi was designed to yield temperature differences with respect to a reference copper-constantan thermocouple mounted close to the resistance-thermometer bulb.

In the experiments reported in reference 1, an accurately scaled aerodynamic model of the present hydrodynamic Venturi was used to define the wall pressure distribution in the critical quarter-round region, which includes the point of minimum pressure. Because of the small size of the region, it was not feasible to install adequate pressure instrumentation on the quarter round of the hydrodynamic Venturi. The range of Reynolds numbers included in the aerodynamic data of reference 1, however, proved inadequate for use in the present study because of the relatively high Reynolds numbers obtained with liquid nitrogen (about four times those for water at the same flow velocity). Further aerodynamic studies, extending these previous data to higher Reynolds numbers, were made with the identical model and experimental arrangement. Model details are presented in reference 1.

Pressure Measurements

Tunnel, bath, and working-section pressures were measured by banks of 7-foot-high multiple-tube mercury manometers. The sealed mercury reservoirs of the manometers were interconnected with the tunnel pressurization system so that all readings were relative to the tunnel pressure measured in the gas space above the liquid nitrogen in the expansion chamber. This reference tunnel pressure was measured by a column of mercury when possible, otherwise by a precision gage. The range of the overall pressure-measuring system limited the operational flow velocity to about 55 feet per second (maximum studied) at the test-section inlet. Manometers were read to within about ±0.03 inch.

The pressure lines leading from the tunnel and the Venturi static taps, through the bath liquid and wall, were arranged horizontally for several inches just inside the bath and continued for at least 1 foot just outside the bath (in air). The horizontal run was located 4 inches above the Venturi centerline. Local pressures within the Venturi ranged from less than to greater than the vapor pressure corresponding to the bath temperature (lowest system temperature). When local Venturi pressures exceeded the vapor pressure corresponding to the bath temperature, a compressed or subcooled liquid (relative to bath conditions) existed in the pressure lines, and the vapor-liquid interface occurred within the horizontal run. Thus, for this condition, a hydrostatic head correction of 4.0 inches of liquid nitrogen was applied to the manometer readings. When indicated pressures were less than the vapor pressure corresponding to the bath temperature, the pressure lines were considered to contain only nitrogen vapor (given sufficient time for any liquid to vaporize), and no hydrostatic head correction was necessary.

Photographic Equipment

Cavitation was photographed by a 4- by 5-inch still camera in conjunction

with either a 0.5- or a 1.2-microsecond high-intensity flash unit. Sixteen-millimeter movies were taken either by a system with a maximum of 6000 frames per second and a synchronized intermittent light source (1 flash/frame) or by a rotating-drum camera (max. speed, 26,000 frames/sec) and a continuous light source with electronically timed flash duration.

PROCEDURE

Facility Operations and Techniques

The liquid nitrogen used in the cavitation studies was commercially obtained in accordance with U.S. Air Force specification MIL-P-27401A but with the following exceptions: nitrogen, greater than 99.99 percent; oxygen, not more than 50 parts per million by volume; and hydrocarbons (taken as methane), not more than 5.0 parts per million by volume. The nitrogen actually used in the study was not analyzed, but random sampling at the Lewis Research Center showed the moisture content to be not more than 15.0 grams per 1000 cubic feet of liquid, a typical value being about 5.0 grams per 1000 cubic feet.

Just prior to the overall cavitation study, the tunnel facility was thoroughly cleaned and dried. For each filling, the facility was first evacuated and sealed under vacuum, and then the supply Dewar was pressurized (4 to 6 lb/sq in. gage) to transfer the liquid nitrogen. Cooldown and filling of the tunnel and the bath required approximately 1 hour; the facility was allowed to cold-soak for an additional hour with the liquid circulating slowly to prevent possible freezing of the pump shaft bearing. The liquid level in the bath was maintained at least 1 inch above the tunnel expansion chamber. The bath liquid was not pressurized, and its temperature was nearly constant at $139.1 \pm 0.2^{\circ}$ R for all studies. Moderate bubbling within the bath liquid did not hinder observation of the test section and could be temporarily suppressed by closing the vent valve. The tunnel liquid temperature was higher than the bath temperature by an amount ranging from about 0.7° F with the pump idle to 4.5° F at the maximum tunnel velocity studied (55 ft/sec). Heat transfer between the tunnel and the bath liquids was not sufficient to remove all the heat imparted to the tunnel liquid by (1) energy input from the pump and (2) a heat leak through the air-exposed impeller shaft and the back side of the pump. Required pressurization of the tunnel liquid was accomplished by admitting dry nitrogen gas to the ullage space in the expansion chamber. During a data run, the flow velocity in the Venturi approach section was fixed, and Venturi cavitation was controlled by varying the gas pressure in the expansion chamber. For a fixed approach velocity, the tunnel liquid temperature did not vary with extent of cavitation.

Criteria and Character of Incipient Cavitation

The operating condition at which the formation or collapse of vapor bubbles near the model surface is just detectable by eye is defined herein as incipient cavitation. Audible detection of incipient cavitation in liquid nitrogen was not attempted. With nitrogen, incipient cavitation was evidenced by intermittent bursts of vapor cavities with leading edges located in the region of minimum pressure on the quarter round. Size and appearance of individual incipient

cavities varied considerably with free-stream velocity, as shown in figure 4. Typical low-speed cavities (20 ft/sec, fig. 4(a)) were about $1\frac{1}{2}$ inches long by $\frac{3}{8}$ inch wide. They began with leading edges in the minimum-pressure region but were quickly swept downstream (center burst, fig. 4(a)). Typical higher speed cavities (39.5 ft/sec, fig. 4(b)) were about 0.2 inch long by 1/8 inch wide with leading edges remaining in the minimum-pressure region. Each burst of incipient cavitation lasted only a short time (order of a few msec). Incipient cavitation never occurred as a complete ring, but, with increasing flow velocity, the cavitation bursts were smaller and more numerous, and the frequency of occurrence increased to several per second. No measurable differences in incipient conditions were observed whether the incipient state was approached from initially noncavitating flow by decreasing pressure (onset method) or by increasing pressure from an initially greater than incipient cavitation state (suppression method). As in the study of reference 1, incipient conditions were based on observations of cavitation at circumferential locations well away from the localized cavitation of pressure taps 2 and 3 (fig. 3).

Determination of Effective Liquid Tension

If a flowing liquid cavitates incipiently when the minimum pressure h_{min} equals the vapor pressure corresponding to the stream liquid temperature h_v, then, in terms of the conventional pressure coefficient C_p and the incipient cavitation parameter K_i, it follows that

$$-C_{p,min} \equiv \frac{h_0 - h_{min}}{V_0^2/2g} = \frac{h_0 - h_v}{V_0^2/2g} \equiv K_i \tag{1}$$

(Symbols are defined in the appendix.) Consequently, an experimentally determined value of K_i less than $-C_{p,min}$ means that h_{min} is less than h_v, or, as defined hereinafter, a condition of effective liquid tension exists within the liquid. For convenience, $K_i + C_{p,min}$ is called the effective-tension parameter. Its value is a measure of tension in terms of the velocity head $V_0^2/2g$. The absolute value of effective liquid tension is computed from the relation

$$h_{min} - h_v = \frac{V_0^2}{2g}(K_i + C_{p,min}) \tag{2}$$

This determination assumes that noncavitating values of $C_{p,min}$ are valid at incipient cavitation or, more exactly, at the single-phase liquid condition just prior to the incipient threshold on the model. Aerodynamic pressure data, corrected to incompressible flow values, are used to obtain values of $C_{p,min}$. For a fixed free-stream velocity V_0, K_i is determined by measuring free-stream values of static pressure h_0 and temperature at incipient conditions; the latter measurement is used to determine free-stream vapor pressure h_v. Free-stream values always refer to conditions within the Venturi approach section (fig. 3(a)).

Measurements of inner-wall temperature in the Venturi approach section ($x = 3.12$ in., fig. 3(a)) indicated no temperature difference from that measured by the platinum resistance thermometer located $14\frac{1}{2}$ inches upstream (fig. 1). Free-stream velocity V_0 was calculated from the static-pressure-head difference across the tunnel contraction nozzle (flow coefficient of unity). Corrections for flow areas at the nozzle taps and dimensional changes that occurred at liquid-nitrogen temperature were considered so that

$$V_0 = 8.21 \sqrt{\Delta h} \tag{3}$$

RESULTS AND DISCUSSION

Noncavitating Pressure Distributions

Typical axial distributions of wall-pressure coefficients for the hydrodynamic and aerodynamic Venturis are presented in figure 5 together with results obtained from computations for incompressible irrotational flow. The computed results are for the actual Venturi shape tested and are identical with those described in detail in reference 1. The experimental data herein are for free-stream Reynolds numbers near 1.68×10^6 (V_0 in liquid nitrogen of about 24 ft/sec), whereas the computed results are for an infinite Reynolds number. A magnified plot of the pressure distribution in the critical minimum-pressure region is presented in the left half of figure 5(a), while the right half of figure 5(a) shows the experimental variation of $C_{p,min}$ with Re_D. The good agreement between aerodynamic, computed, and liquid-nitrogen results in the minimum-pressure region validates the use herein of aerodynamic values of $C_{p,min}$ as a function of Re_D in the determination of minimum pressure at incipient cavitation. Faired $C_{p,min}$ values range from -3.20 at an Re_D of 0.23×10^6 to -3.50 at an Re_D of 1.63×10^6 (max. Re_D obtainable in the wind tunnel). The minimum computed value of $C_{p,min}$ is -3.82. The location of $C_{p,min}$ was at an x/D of 2.471 (66° of arc) and did not change with Re_D. (An auxiliary scale of liquid-nitrogen stream velocity is included with the $C_{p,min}$ plot (fig. 5(a)) for convenience.)

The axial distribution of wall-pressure coefficient for the complete Venturi, including the approach section, is presented in figure 5(b) for the same conditions as those of figure 5(a).

Incipient Cavitation

The incipient-cavitation parameter K_i for the Venturi in nitrogen is presented in figure 6 as a function of free-stream velocity. The negative noncavitating $C_{p,min}$ values (from fig. 5(a)) are plotted for reference, as is the limiting computed value of $-C_{p,min}$ at infinite Reynolds number. Values of K_i are always considerably less than $-C_{p,min}$, an indication (from eq. (1)) that, at incipient cavitation, the minimum pressure h_{min} on the Venturi is always less than the free-stream vapor pressure h_v. With increasing free-stream velocity, K_i steadily increases, and at the higher speeds the K_i curve almost

parallels the $-C_{p,min}$ curve.

A comparison of liquid-nitrogen incipient-cavitation results with the visible incipient-cavitation results for water in the identical Venturi (ref. 1) is presented in figure 7, where K_i is plotted as a function of free-stream Reynolds number based on liquid properties corresponding to the free-stream temperature at each condition. The use of Re_D is merely for convenient reference and is not intended to demonstrate the usefulness of Re_D as a correlating factor. The visible K_i values for water (from ref. 1) represent data for demineralized, distilled, and tap water studied over a wide range of air content. The range of free-stream velocity for the water data is 19 to 45 feet per second and that for liquid nitrogen is 17 to 55 feet per second. Although incipient cavitation in nitrogen was readily detected, it was less abrupt and less consistent compared with that in water; consequently, the nitrogen data show a little more scatter than the water data. The K_i values for nitrogen steadily increase with increasing Reynolds number, whereas values of K_i for water tend to become asymptotic to a value near 2.75. Except at the highest speed (highest Re_D), the nitrogen K_i values are all less than the minimum value of K_i measured in water ($K_i \approx 2.4$). For the same speed, the greatest difference between nitrogen and water K_i values occurs in the low-speed (low Re_D) range studied with each liquid. Lower K_i values mean more resistance to cavitation; thus, for the conditions investigated, the data of figure 7 show that liquid nitrogen is more resistive to cavitation than water.

The reasons why the nitrogen K_i values are less than those for water are not known. Factors usually considered as affecting K_i are nuclei content and gas content of the liquid, wall nuclei, and fluid properties. All these factors are different for nitrogen and water, and only the differences in fluid properties are known quantitatively. Which of these factors may be controlling the difference between nitrogen and water K_i values can only be surmised at present. Varying nuclei and air content of water did not affect the K_i values (ref. 1). Also, the K_i data for nitrogen in figure 7, which represent seven loadings of the Dewar and the tunnel, indicated no trends due to possible variations in nuclei or gas content. The gas content for all the nitrogen data is less than the minimum studied for water (about 6 percent saturated, see ref. 1). If the gases in both liquids are not completely dissolved, this may help to lower nitrogen K_i values relative to water. It is possible that any Venturi wall nuclei may be somewhat lower at liquid-nitrogen temperatures than at water temperatures, which in turn may result in lower K_i values for nitrogen compared with water. Considering the preceding observations, the difference between the nitrogen and the water K_i values of figure 7 is presently attributed to differences in fluid properties. The study of additional liquids in the same Venturi is required to substantiate the importance of the effect of fluid properties on K_i and to indicate which properties may be the controlling ones.

The liquid-nitrogen data of figure 7 are plotted in figure 8 in terms of the effective-tension parameter $(h_{min} - h_v)/(V_o^2/2g)$ and effective liquid tension $h_{min} - h_v$. The corresponding results for water are included for comparison. The effective-tension parameter measured in liquid nitrogen varied, in a continuous manner, from -1.7 at low velocity to a minimum (less negative) value of about -1.24 at 55 feet per second, whereas the curve for water shows a knee at about

30 feet per second beyond which there is little variation with further increasing velocity. In terms of feet of the particular liquid (lower half of fig. 8), the values of effective tension obtained for nitrogen are about twice those for water for a given free-stream velocity. For liquid nitrogen the effective tension ranges from 8 to 60 feet at stream velocities of 17 to 55 feet per second, respectively. It may be observed from figure 8, as well as from the water data of reference 1, that the effective tension calculated at the visible inception of cavitation increases as free-stream velocity increases. This is consistent with the idea that the growth of a moving nucleus to the visible size of incipient cavitation is in some manner dependent upon both the length of time the fluid is exposed to local pressures less than the stream vapor pressure and the magnitude of these pressure depressions. The length of time below the stream vapor pressure is called nucleation or exposure time herein. The method used to calculate exposure times is given in reference 1. It should be noted that during the exposure time the flowing fluid experiences pressure decrements relative to the vapor pressure that vary between zero and the maximum values presented (effective liquid tension). (A scale of liquid-nitrogen exposure time is included at the bottom of fig. 8 for reference.) Unfortunately, exposure time and effective tension are interrelated and are functions of pressure distribution, free-stream velocity, and the incipient-cavitation parameter, which, in turn, can be affected by the several factors previously discussed. With additional systematic experimental studies of different liquids flowing through various pressure distributions (various model shapes and scales), however, it may be possible to deduce a reasonably correct K_i value or trend for an arbitrary body and liquid by means of some relations between effective tension and exposure time. This approach might be aided by other comprehensive experimental tension-time studies with static liquids.

Effects of Cavitation on Local Temperatures and Pressures

In noncavitating flow, liquid temperatures are uniform throughout the Venturi; however, when the liquid ruptures, or cavitates, a phase change occurs because the voids rapidly fill with vapor. Vapor generation involves the heat of vaporization, which must be drawn from the surrounding liquid. Vapor generation should result in a cooling of the vapor-liquid interface and in a reduction in temperature around and within the cavity. If conditions within the cavity are in thermodynamic equilibrium, the pressure should drop to the vapor pressure corresponding to the reduced local temperature.

As an initial step in evaluating some of the thermodynamic effects of cavitation, nominally fixed amounts of cavitation were generated in nitrogen, and the stabilized temperatures and pressures within the cavitated region were measured.

Figure 9 shows pressure and temperature variations within the cavitated nitrogen region as functions of axial distance for three extents of cavitation at a nominal free-stream velocity of 20 feet per second. Photographs taken simultaneously with the pressure and temperature measurements are shown in figure 10. Well-developed cavitation extended to about 1, 2, and 4 inches ($\pm 1/2$ in.) as shown in parts (a), (b), and (c), respectively, of figures 9 and 10. Beyond these points, collapse occurred. Even within the region of

well-developed cavitation a frothy and rapidly varying mixture of vapor and liquid existed; thus, measured temperatures and pressures reflect time-average values of the mixture and not conditions within a purely vaporous cavity. The solid curve through the circles in figure 9 represents pressures measured directly by the Venturi wall taps, while the horizontal line represents the vapor pressure corresponding to the free-stream (liquid) temperature of 140.0° R. Within the region of well-developed cavitation, measured pressures are less than the vapor pressure corresponding to the free-stream liquid temperature, the maximum reduction being about 5 feet of liquid nitrogen for a velocity of 20 feet per second. The start of the collapse regions (fig. 10) closely coincides with the points where the measured pressure curves cross the free-stream vapor pressure line (fig. 9). Farther downstream the pressures continually increase and approach the noncavitating values shown by the dashed line (except for head losses), although the photographs show numerous collapsing vapor cavities within this region. Pressure measurements from taps 2 and 3 (fig. 3) are not presented. The axial distance of these taps from the point of minimum pressure is less than 0.1 inch and because of the ragged and erratic location of the leading edge of cavitation, especially at the higher speeds, these two pressure measurements were not considered representative of a cavitated region.

The square symbols in figure 9 represent values of vapor pressure that correspond to the measured temperatures, which range from 138.2° to 139.9° R. Within the region of well-developed cavitation, the vapor pressures corresponding to these measured temperatures are in reasonable agreement with the local static pressures measured directly; thus thermodynamic equilibrium appears to exist. The pressures within the cavitated region correspond to vapor pressures at locally reduced or depressed temperatures and not to the vapor pressure at the free-stream liquid temperature, as might be first assumed. The axially decreasing pressure and temperature depressions below the free-stream vapor pressure and temperature reflect the adverse pressure gradient (fig. 5), which reduces the cavity growth rate and thus reduces the evaporative cooling effect. The larger temperature (and pressure) depressions with increasing amounts of cavitation are attributed to a local increase in the vapor volume, which requires more latent heat extraction from the neighboring liquid. For conditions presented in figure 9, the minimum pressure (located at an axial distance of zero) at, or just prior to, incipient cavitation was 33 feet of liquid nitrogen absolute.

Temperature and pressure depressions also increased with free-stream velocity at fixed length or extent of cavitation. Figures 11 and 12 show, respectively, the pressure variation with a nominal $4\frac{1}{2}$-inch-long cavity and the corresponding photographs for a range of V_0 from 25.1 to 42.0 feet per second. As before, there is approximate agreement between the start of collapse in the photographs (fig. 12) and the point where the measured pressure curve crosses the free-stream vapor-pressure line (fig. 11). The level of stream vapor pressure increases with tunnel speed because of the additional heat added by the pump. There is reasonable agreement between measured pressures and vapor pressures corresponding to measured temperatures, except within the first 5/8 inch of axial distance at the higher speeds. As speed increases, the leading edge of cavitation becomes more erratic and ill-defined and tends to move farther downstream from the minimum-pressure region (fig. 12). Axial and circumferential locations of the leading edge fluctuate considerably; thus, fixed flaws or solid particles

are not considered to be the cause of the behavior shown in figure 12. The cavity growth time is apparently too marginal at the higher speeds to assure a well-defined leading edge. Because of the discontinuous nature of the cavity within the 5/8-inch region, the curve representing measured pressures is not extended into this region. From figure 11, the maximum temperature depression (below the free-stream value) measured within the well-developed cavitation region is 3° F at a free-stream velocity of 42 feet per second. A 3° F temperature drop corresponds to a vapor pressure depression of 9 feet of liquid nitrogen.

For a fixed cavity length, the larger temperature (and pressure) depressions shown in figure 11 at the higher flow velocities are rationalized as follows. The fluid approaching the cavitation zone experiences some pressure decrement below the stream vapor pressure because of finite times required for bubble nucleation. The value of this pressure decrement cannot be readily determined because of unknown changes in the pressure distribution upstream of the well-developed cavitation, but the decrement most likely increases with flow velocity. Thus, at the instant that vaporization (flashing) takes place, there is a greater driving potential (pressure decrement or liquid superheat) at the higher speeds, and increased rates of vaporization result. For a fixed cavity length (implying fixed cavity volume), therefore, approximately the same mass or volume of liquid is vaporized at the different speeds, but in shorter times as speed increases. Consequently, with increasing speed, the latent heat is probably drawn from a smaller mass (thickness) of liquid, and thus, a larger temperature depression is produced.

For nitrogen, the maximum temperature depressions measured (and the equivalent pressure depressions) are summarized in figure 13 for nominal cavitation lengths of $1\frac{1}{2}$ and $4\frac{1}{2}$ inches over a speed range of 20 to 45 feet per second. Temperature depressions increase with length of cavitation and speed, and range from 1° to 3° F (3 to 9 ft of liquid nitrogen). For nearly room temperature water and conditions comparable to those just presented for liquid nitrogen, measured temperature depressions ranged from less than 0.1° to about 0.3° F. Changes in vapor pressure due to these small temperature depressions are insignificant; thus, pressures within the cavitated regions in water are essentially the vapor pressure at the free-stream liquid temperature. The low values of temperature depression measured in water, as compared with nitrogen, were anticipated. For a given cavity volume, the heat required for vaporization (product of vapor density, latent heat, and volume) is many times less for water than for nitrogen, the very low density of water vapor being the controlling factor.

General Comparisons of Cavitation in Nitrogen and Water

Many of the observations of cavitation of water reported in reference 1 apply to the cavitation of nitrogen, except that herein no variations in gas content, purity of liquid, or noise level were investigated. The following major differences in cavitation characteristics of nitrogen and water in the same Venturi were observed: (1) at all magnitudes of nitrogen cavitation, the process was much less violent than for water; (2) rates of cavity formation in nitrogen appear to be much slower than in water, while rates of collapse may be comparable (based on collapse-region lengths for similar axial pressure gradients); and

(3) at the higher speeds, nitrogen incipient cavitation (fig. 4(b)) tends to resemble in size that previously reported for water over a range of speeds.

Comparisons at the same value of K are limited because the minimum K attainable for water (profuse cavitation and tunnel choking) is about 2.2, a value generally higher than K_i for nitrogen, as shown in figure 7. Photographs of nitrogen and water cavitation at a K of 2.34 and comparable speeds are shown in figure 14. Nitrogen is at incipient conditions, while the water contains extensive cavitation. Obviously, K does not predict the same degree of cavitation between water and nitrogen, a fact which others have recognized and which has led to the proposal that other correlating factors might account for the thermodynamic effects of cavitation (refs. 7 to 9). Temperature and pressure depressions within the cavitated region tend to limit cavity growth, and, as previously indicated, such depressions were significant in liquid nitrogen but negligible in water. Thus, nitrogen requires a lower K than water for comparable extents of cavitation. For example, a nitrogen K of 1.7 gives the same extent of cavitation as for the water shown in figure 14(b) at a K of 2.34.

For the Venturi studied, a constant K of 1.78 produced a nearly constant $1\frac{1}{2}$- to 2-inch-long nitrogen cavity over a V_o range from 20 to 45 feet per second. On the other hand, with water, equal lengths of cavitation were more nearly a function of $K_i - K$. These criteria, however, did not suffice for all extents of cavitation over the full speed range.

SUMMARY OF RESULTS

Experimental studies of liquid-nitrogen cavitation in a Venturi over a range of velocities in a small closed-return tunnel yielded the following principal results:

1. Local minimum wall pressures, always significantly less than the vapor pressure corresponding to the free-stream liquid temperature, were obtained at, or just prior to, incipient cavitation. The maximum pressure decrement, or effective liquid tension, ranged from 8 feet of liquid nitrogen at a free-stream (approach) velocity of 17 feet per second to 60 feet of liquid nitrogen at a stream velocity of 55 feet per second.

2. Temperatures and pressures measured within a well-developed cavitation region were in thermodynamic equilibrium but were less than the free-stream values of temperature and vapor pressure. Measured temperature depressions were as high as 3° F and corresponded to a head depression of 9 feet of liquid nitrogen (at the temperatures studied). These depressions increased with both stream velocity and extent of cavitation.

3. Compared with room-temperature water, nitrogen sustained nearly twice the effective tension, always cavitated a lesser amount for a given value of cavitation parameter, and yielded temperature depressions within a cavitated region that were at least an order of magnitude greater: 1° to 3° F for nitrogen compared with 0.1° to 0.3° F for water.

4. Incipient cavitation occurred as intermittent bursts of vapor pockets in the region of minimum pressure. For appreciable amounts of cavitation at higher stream velocities, the upstream edge of cavitation tended to move randomly as much as 5/8 inch downstream from the minimum-pressure location.

Lewis Research Center
National Aeronautics and Space Administration
Cleveland, Ohio, September 19, 1963

APPENDIX - SYMBOLS

C_p	noncavitating pressure coefficient, $(h_x - h_0)/(V_0^2/2g)$, dimensionless
$C_{p,min}$	noncavitating minimum-pressure coefficient, $(h_{min} - h_0)/(V_0^2/2g)$, dimensionless
D	free-stream diameter; for cavitation model, 1.743 in.; for aerodynamic model, 8.03 in.
g	acceleration due to gravity, ft/sec^2
Δh	static-pressure difference across tunnel contraction nozzle, ft of liquid nitrogen
h_{min}	minimum static pressure, ft of liquid abs
h_v	vapor pressure corresponding to free-stream liquid temperature measured by platinum resistance thermometer, ft of liquid abs
h_x	static pressure at x/D, ft of liquid nitrogen abs
h_0	free-stream static pressure at x/D of 1.98, ft of liquid abs
K	cavitation parameter, $(h_0 - h_v)/(V_0^2/2g)$, dimensionless
K_i	incipient-cavitation parameter, $\left[(h_0 - h_v)/(V_0^2/2g)\right]_{incipient}$, dimensionless
Re_D	free-stream Reynolds number based on diameter D, dimensionless
V_0	free-stream velocity at x/D of 1.98, ft/sec
x	axial distance from Venturi inlet, in.
y	radial distance from approach-section wall, in.

REFERENCES

1. Ruggeri, Robert S., and Gelder, Thomas F.: Effects of Air Content and Water Purity on Liquid Tension at Incipient Cavitation in Venturi Flow. NASA TN D-1459, 1963.

2. Kermeen, R. W., McGraw, J. T., and Parkin, B. R.: Mechanism of Cavitation Inception and the Related Scale-Effects Problem. Trans. ASME, vol. 77, no. 4, May 1955, pp. 533-541.

3. Crump, S. F.: Determination of Critical Pressures for the Inception of Cavitation in Fresh and Sea Water as Influenced by Air Content of the Water. Rep. 575, David W. Taylor Model Basin, Oct. 1949.

4. Ziegler, G.: Tensile Stresses in Flowing Water. Cavitation in Hydrodynamics - Proc. of Symposium, Nat. Phys. Lab., Sept. 14-17, 1955.

5. Sarosdy, L. R., and Acosta, A. J.: Note on Observations of Cavitation in Different Fluids. Paper 60-WA-83, ASME, 1961.

6. Wilcox, W. W., Meng, P. R., and Davis, R. L.: Performance of an Inducer-Impeller Combination at or Near Boiling Conditions for Liquid Hydrogen. Vol. 8 of Advances in Cryogenic Eng., K. D. Timmerhaus, ed., Plenum Press, 1963, pp. 446-455.

7. Stahl, H. A., and Stepanoff, A. J.: Thermodynamic Aspects of Cavitation in Centrifugal Pumps. Trans. ASME, vol. 78, no. 8, Nov. 1956, pp. 1691-1693.

8. Salemann, Victor: Cavitation and NPSH Requirements of Various Liquids. Jour. Basic Eng. (Trans. ASME), ser. D, vol. 81, no. 2, June 1959, pp. 167-180.

9. Jacobs, R. B.: Prediction of Symptoms of Cavitation. Jour. Res. Nat. Bur. Standards, sec. C, vol. 65, no. 3, July-Sept. 1961, pp. 147-156.

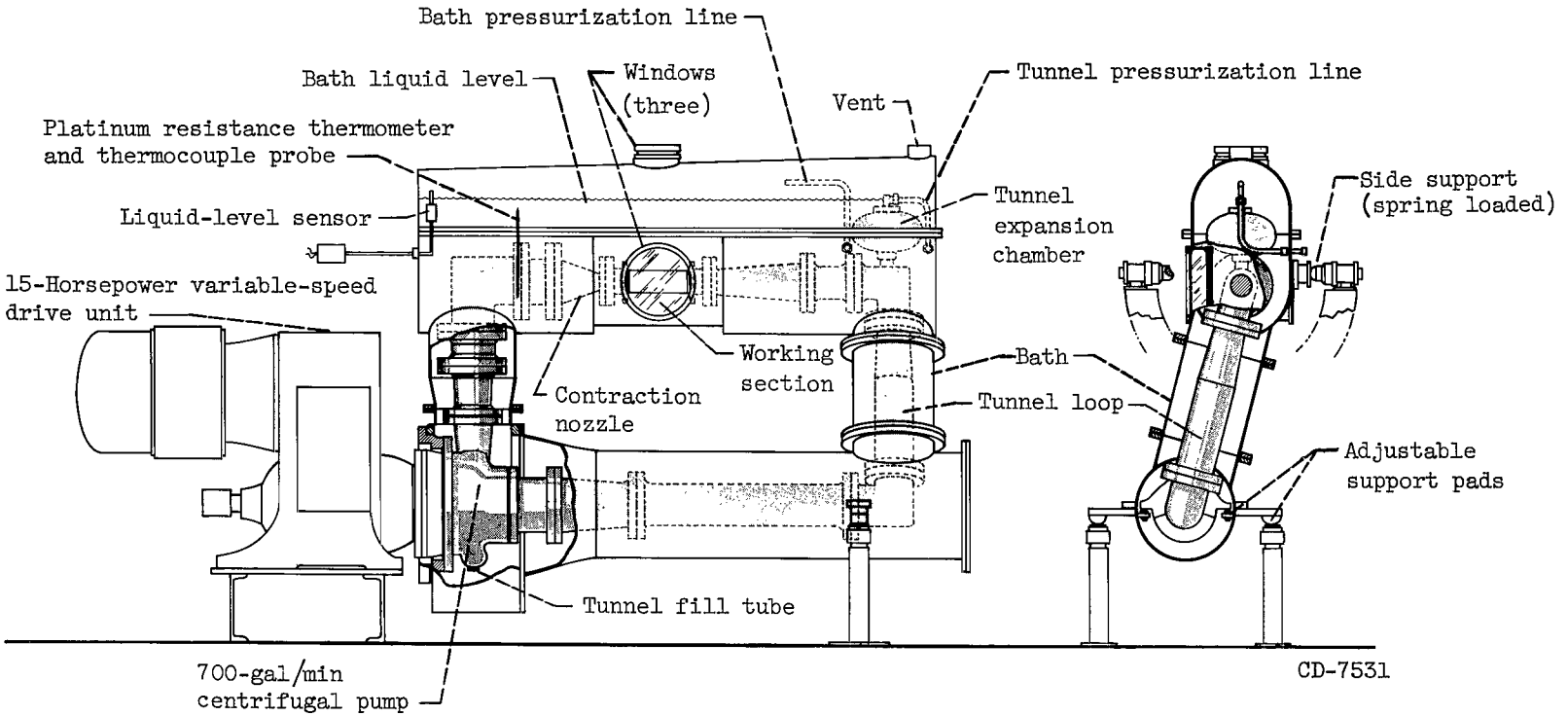

(a) Schematic drawing showing overall tunnel-bath arrangement for liquid-nitrogen operation.

Figure 1. - Cryogenic cavitation tunnel facility.

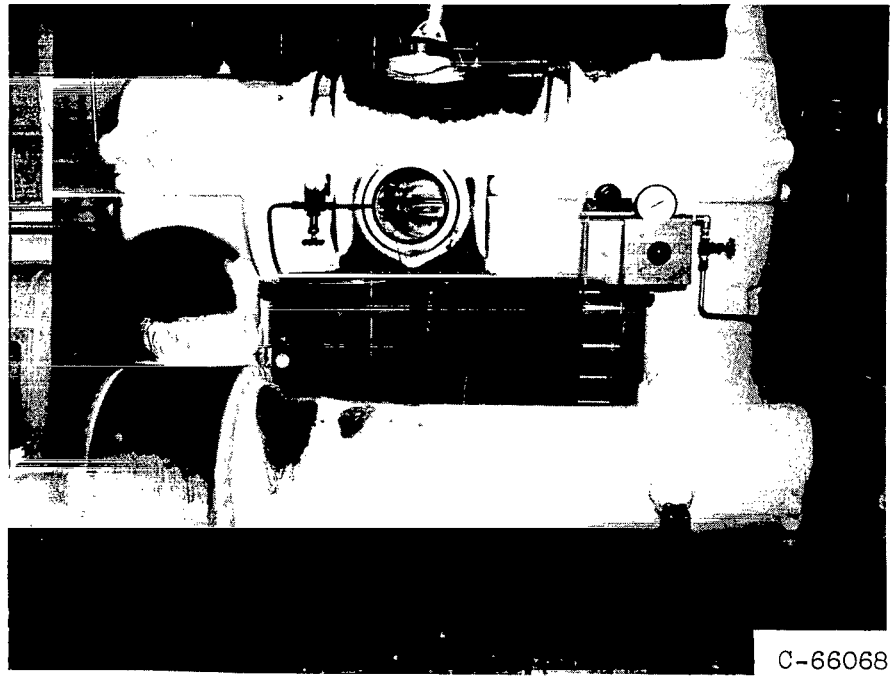

(b) Facility in operation with liquid nitrogen.

Figure 1. - Continued. Cryogenic cavitation tunnel facility.

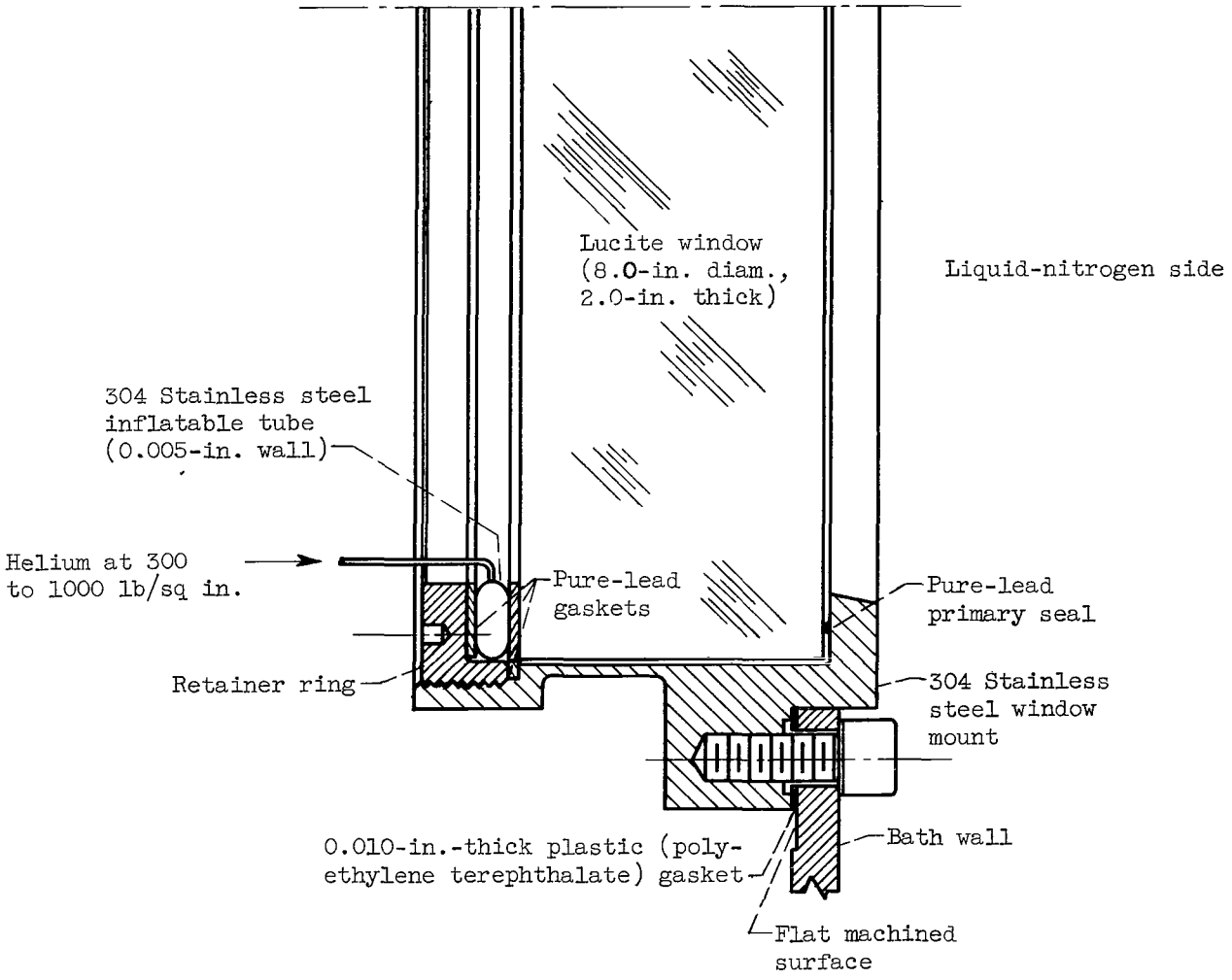

(c) Window details.

Figure 1. - Concluded. Cryogenic cavitation tunnel facility.

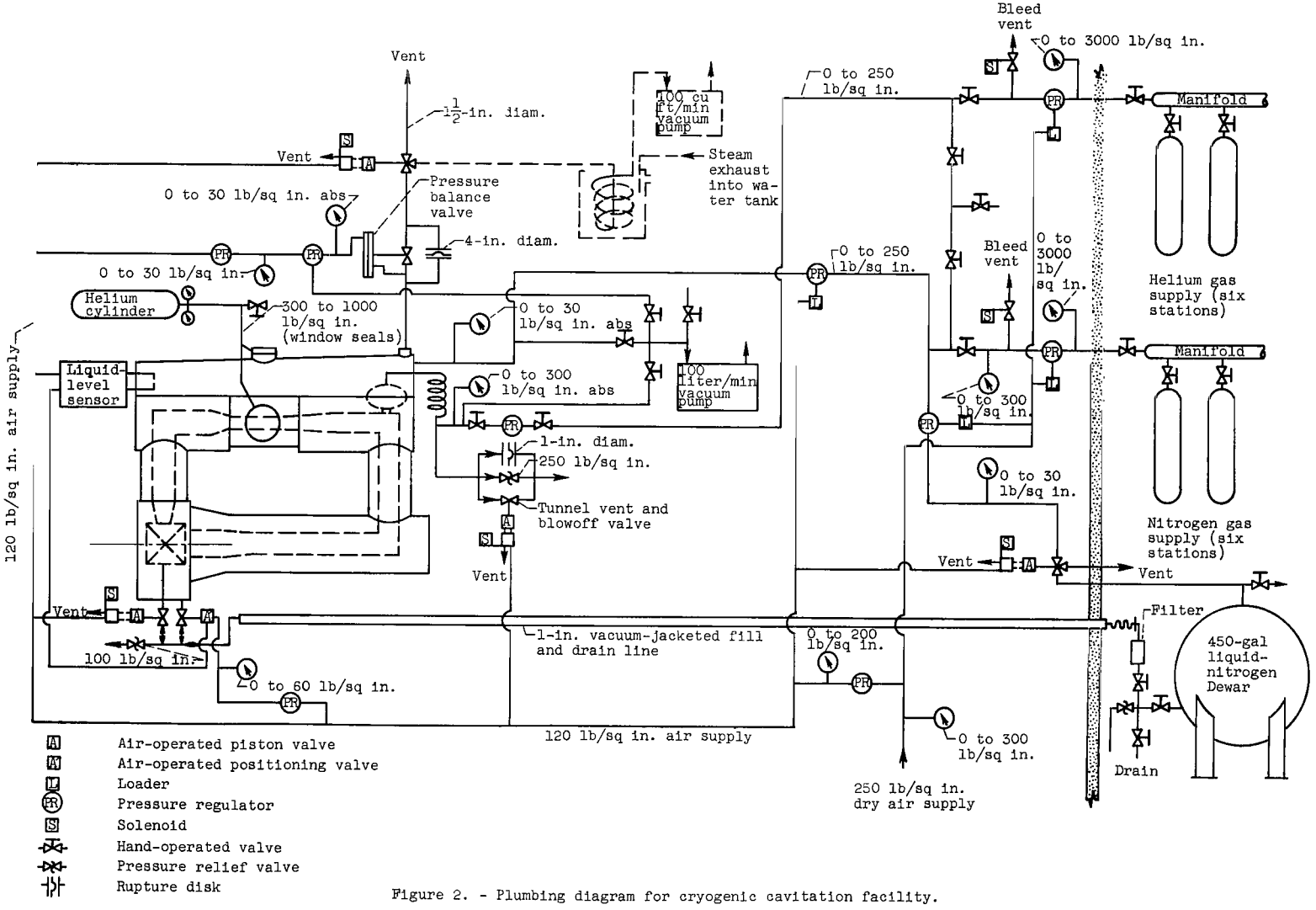

Figure 2. - Plumbing diagram for cryogenic cavitation facility.

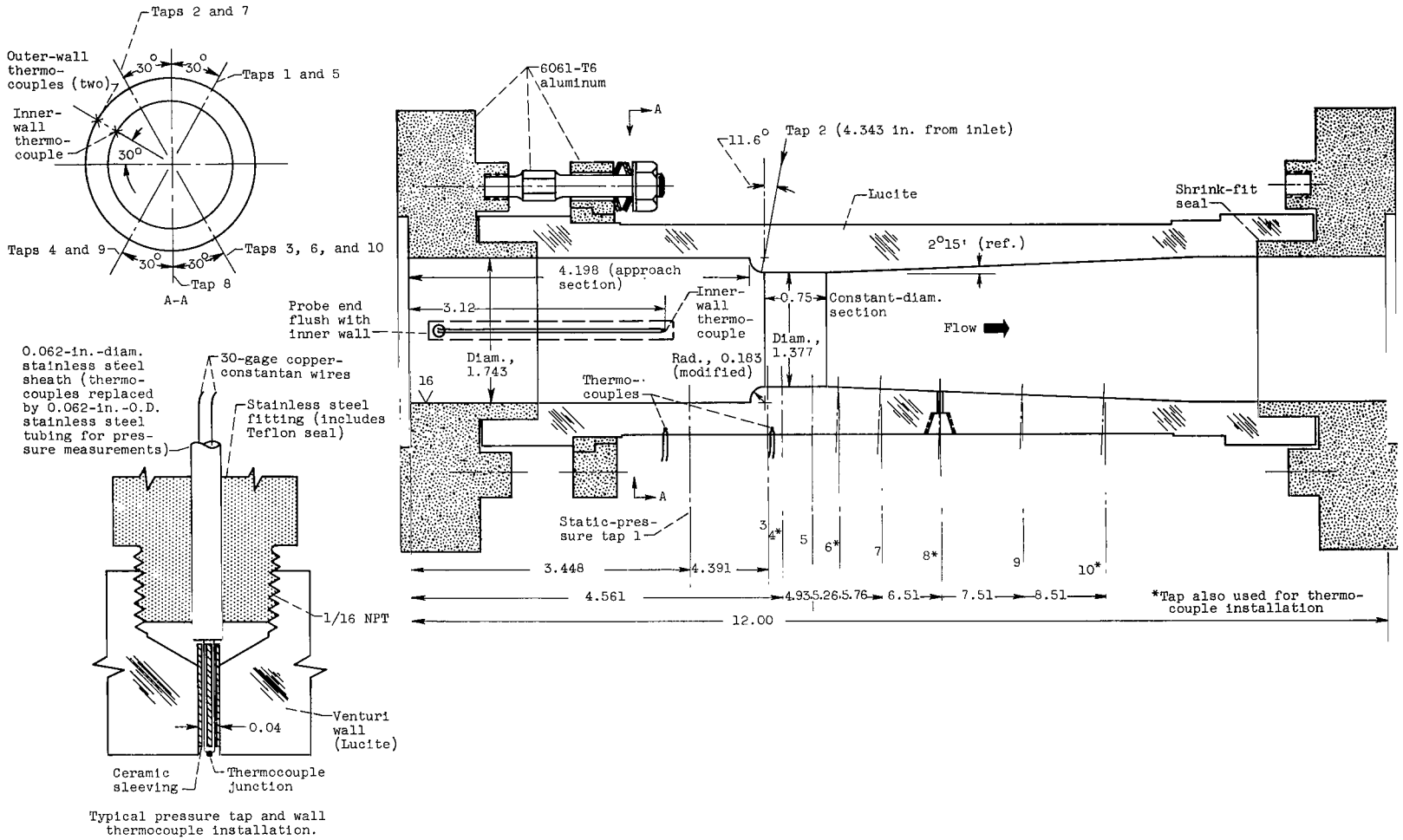

Typical pressure tap and wall thermocouple installation.

(a) Sketch showing dimensions and instrumentation. (Dimensions in inches.)

Figure 3. - Venturi test section.

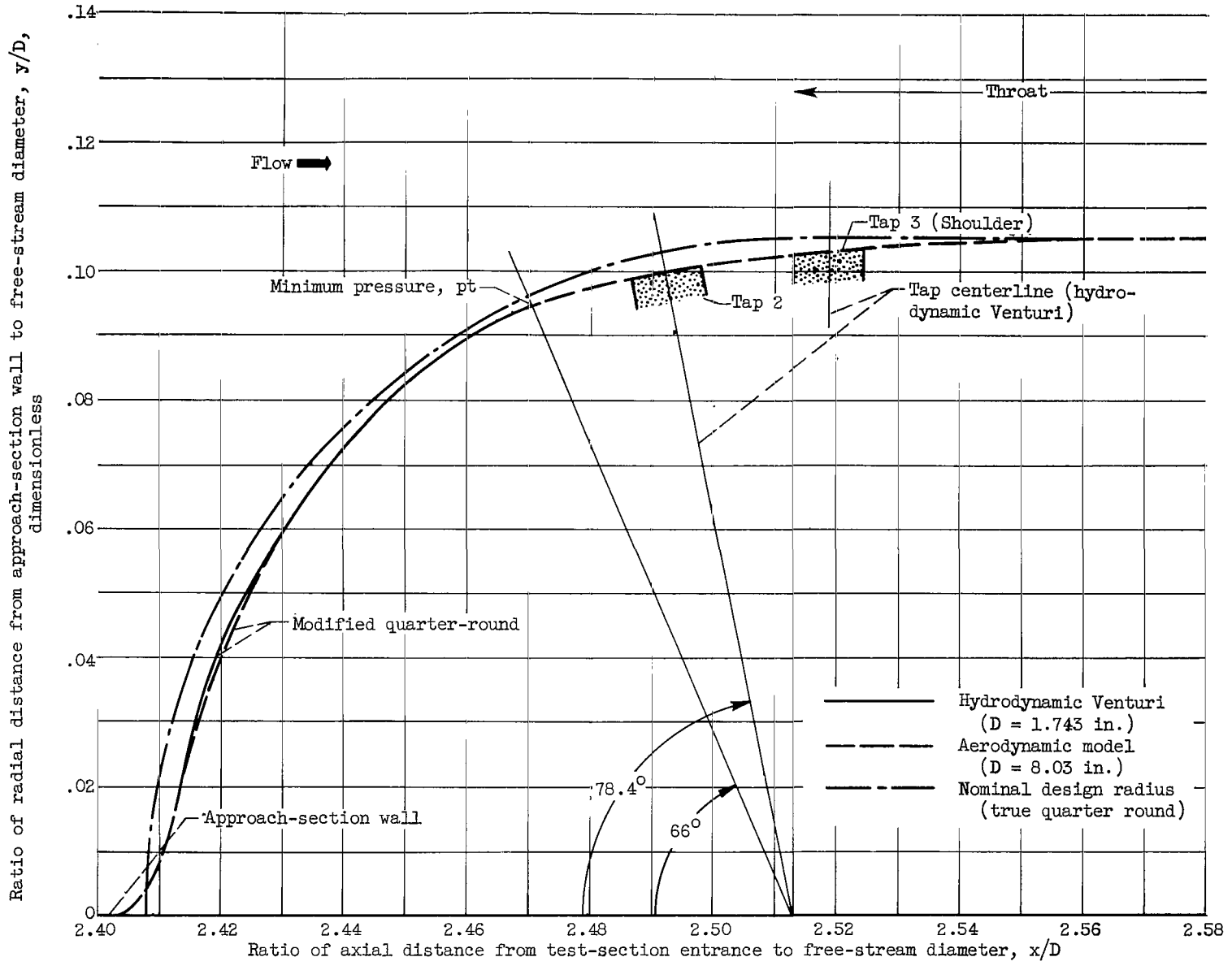

(b) Contour of quarter-round regions for hydrodynamic and aerodynamic Venturi sections.

Figure 3. - Concluded. Venturi test section.

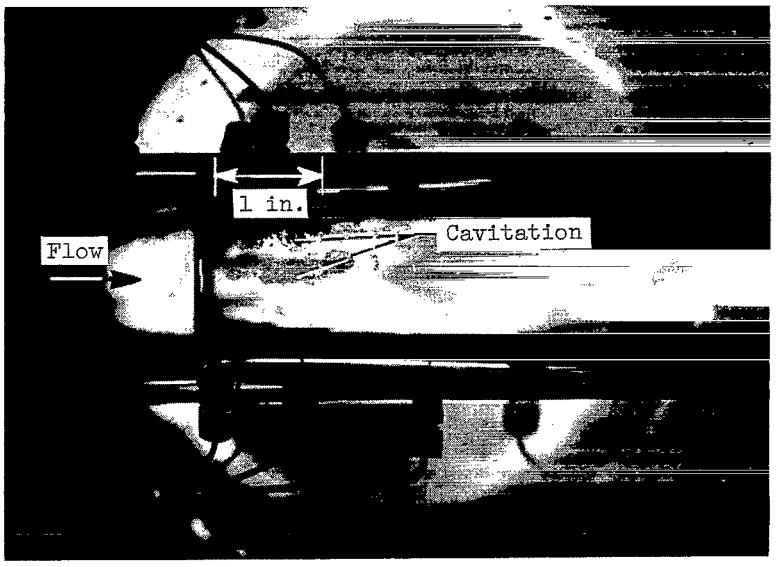

(a) Free-stream velocity, 20.7 feet per second; free-stream temperature, 140.3° R; incipient-cavitation parameter, 1.74.

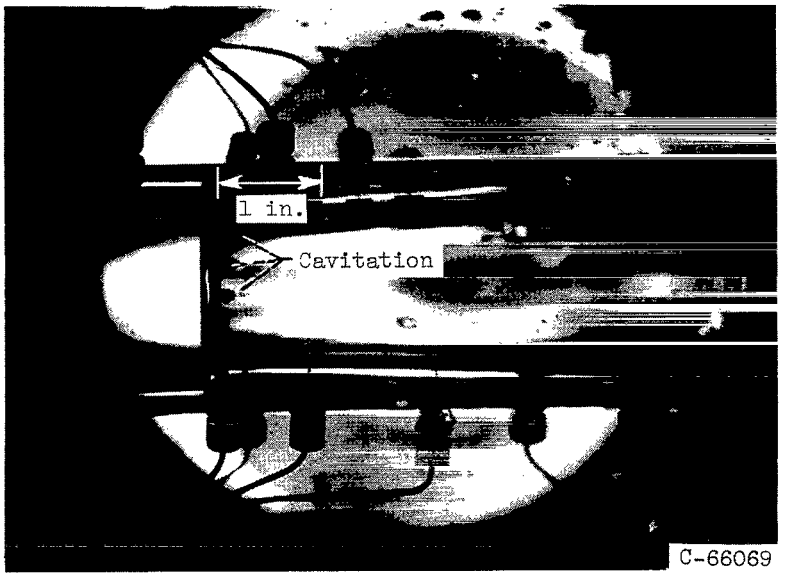

(b) Free-stream-velocity, 39.5 feet per second; free-stream temperature, 141.9° R; incipient-cavitation parameter, 2.22.

Figure 4. - Variation in incipient-cavitation characteristics with free-stream velocity for liquid nitrogen.

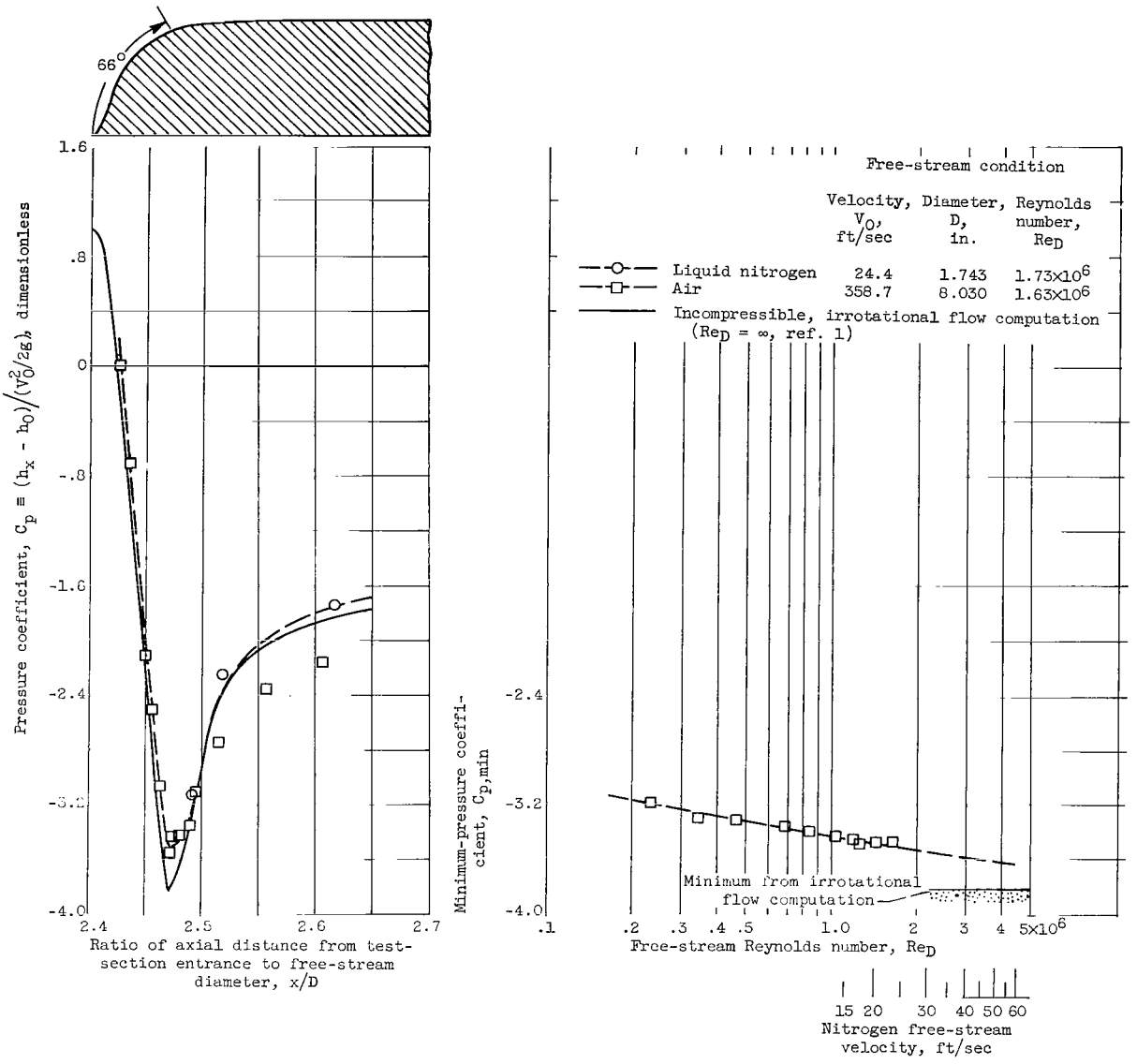

(a) Magnified plot of low-pressure region and variation of noncavitating minimum pressure coefficient with free-stream Reynolds number.

Figure 5. - Noncavitating pressure distribution for liquid-nitrogen and aerodynamic Venturis and comparison with incompressible, irrotational flow computations.

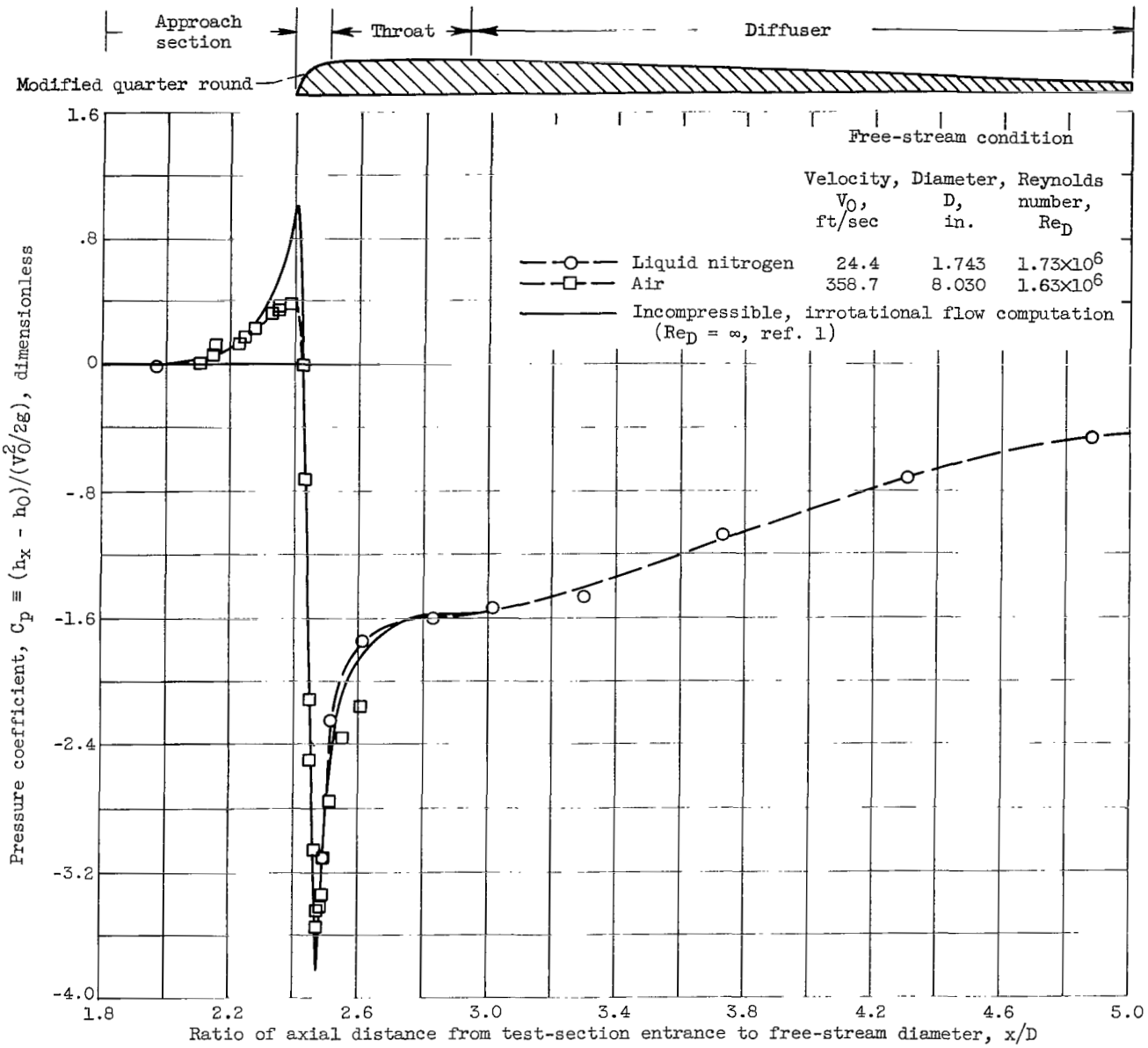

(b) Complete pressure distribution.

Figure 5. - Concluded. Noncavitating pressure distribution for liquid nitrogen and aerodynamic Venturis and comparison with incompressible, irrotational flow computations.

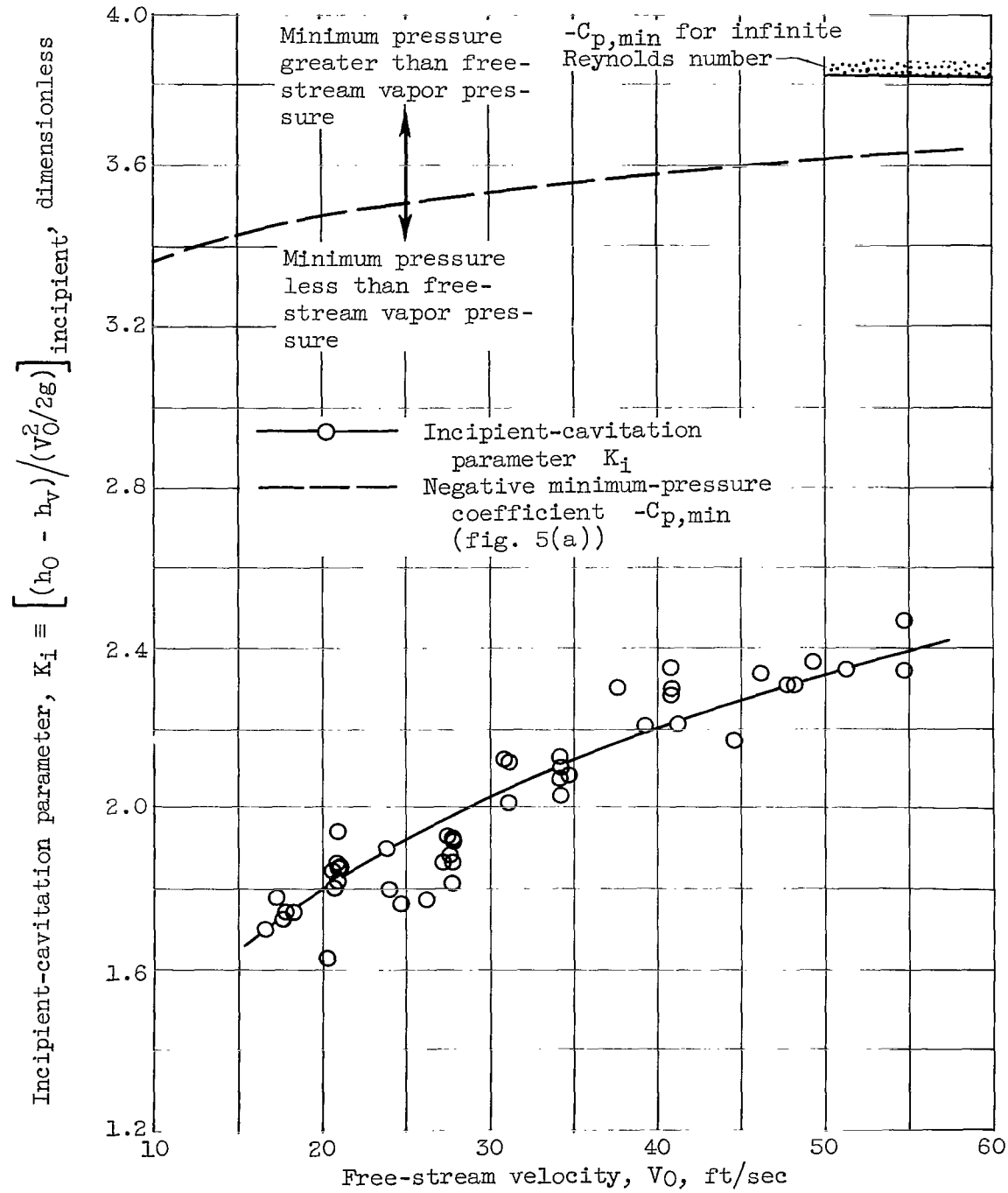

Figure 6. - Incipient-cavitation parameter for nitrogen as function of free-stream velocity.

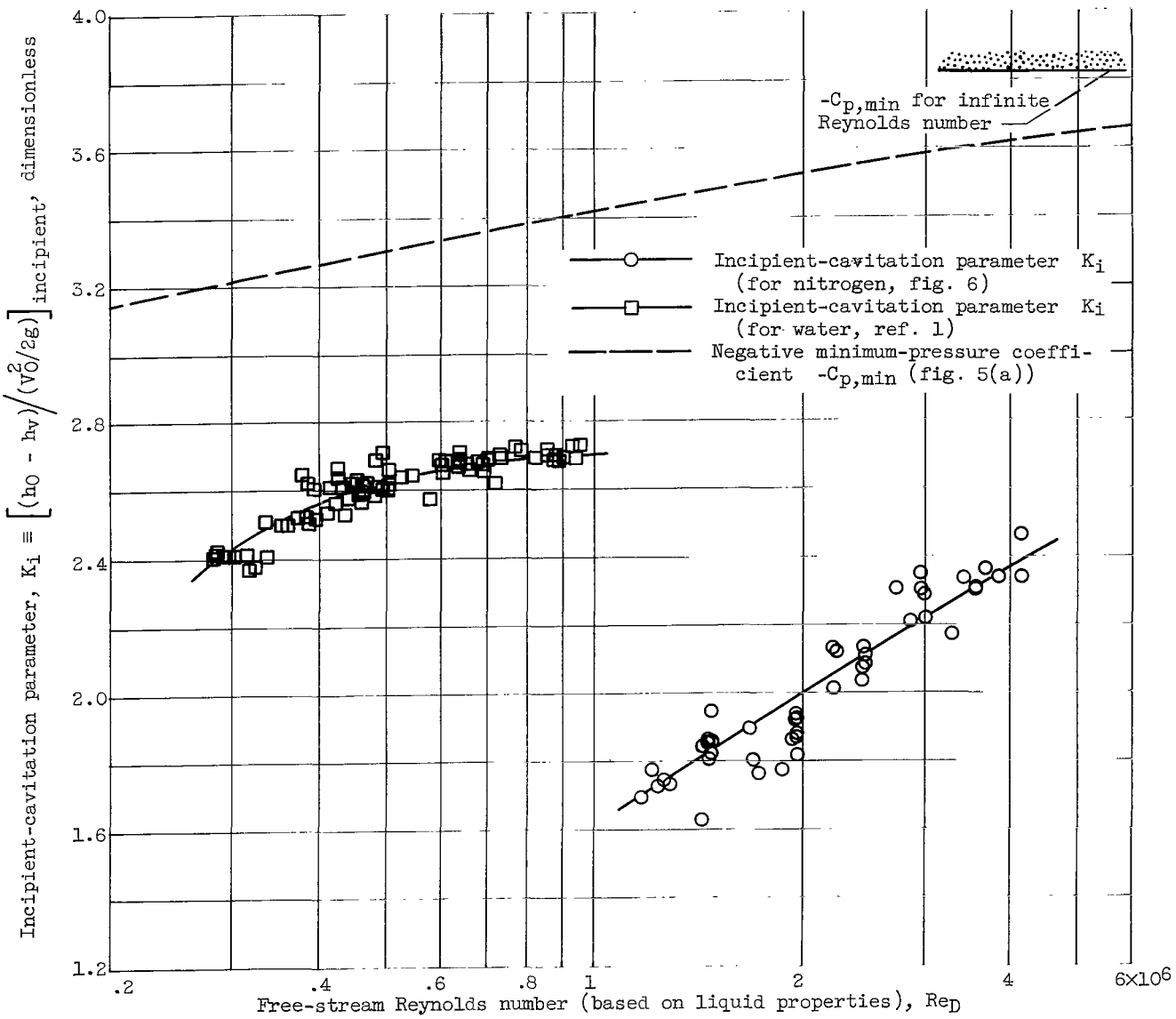

Figure 7. - Comparison of incipient-cavitation parameter for nitrogen and water flowing through same Venturi model.

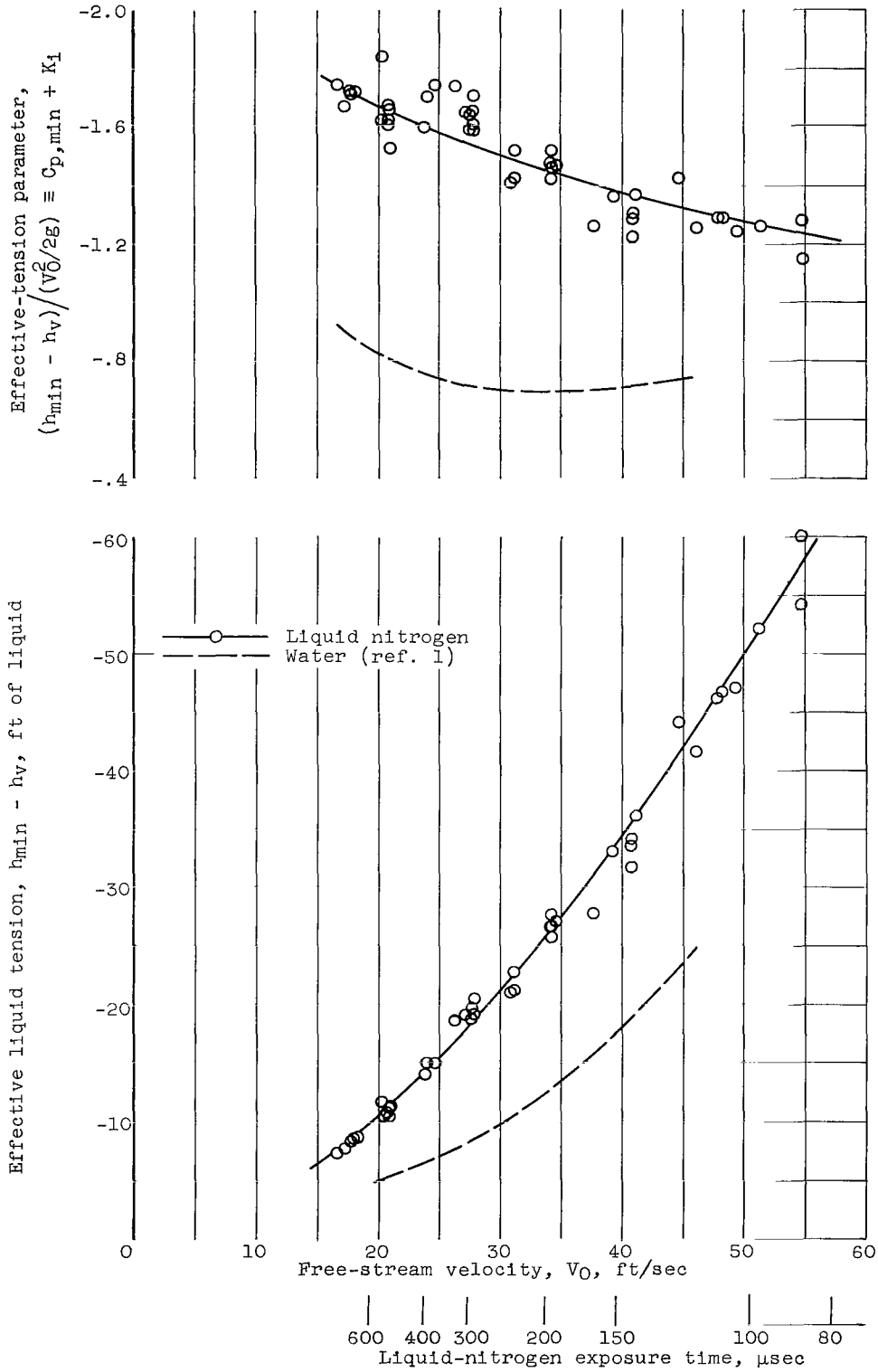

Figure 8. - Effective liquid tension based on visible incipient cavitation.

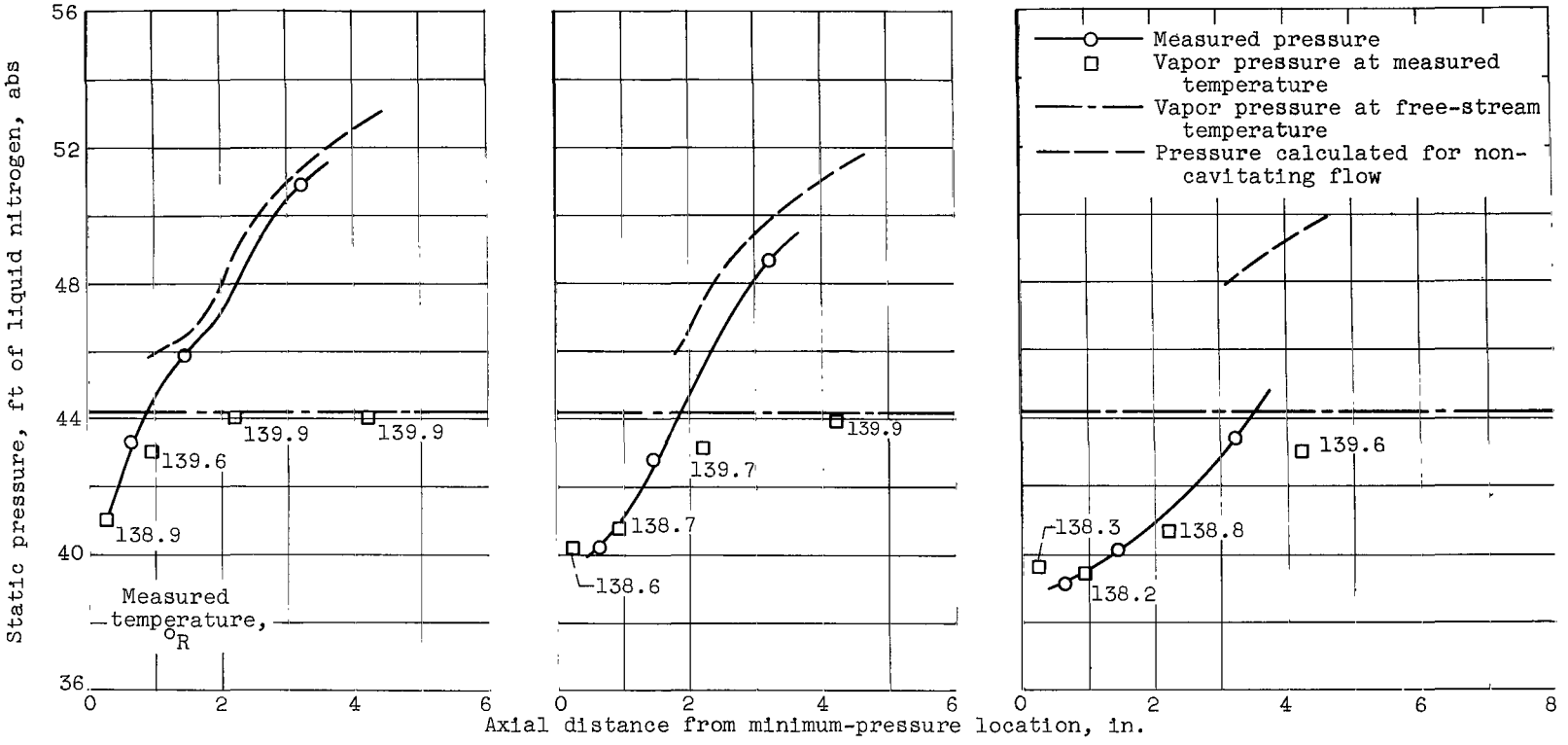

(a) Free-stream velocity, 20.4 feet per second; cavitation parameter, 1.78; nominal cavity length, 1 inch.

(b) Free-stream velocity, 20.1 feet per second; cavitation parameter, 1.61; nominal cavity length, 2 inches.

(c) Free-stream velocity, 19.2 feet per second; cavitation parameter, 1.37; nominal cavity length, 4 inches.

Figure 9. - Effect of cavitation extent on pressure and temperature within cavitated nitrogen region. Free-stream liquid temperature, 140.0° R.

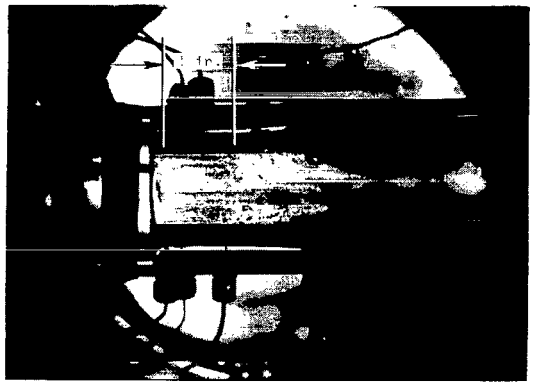

(a) Free-stream velocity, 20.4 feet per second; cavitation parameter, 1.78.

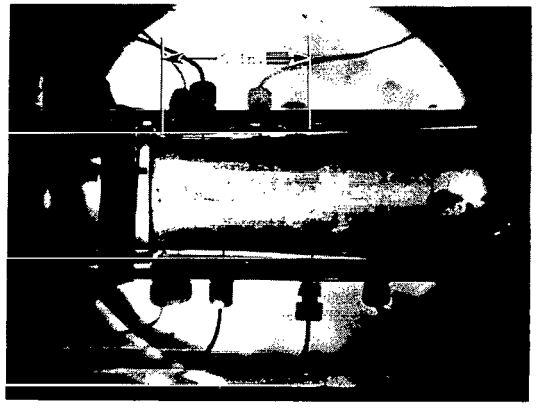

(b) Free-stream velocity, 20.1 feet per second; cavitation parameter, 1.61.

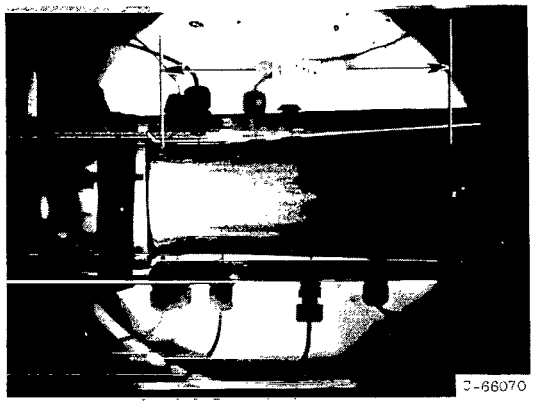

(c) Free-stream velocity, 19.2 feet per second; cavitation parameter, 1.37.

Figure 10. - Effect of decreasing cavitation parameter on extent of nitrogen cavitation. Pictures correspond to data in figure 9.

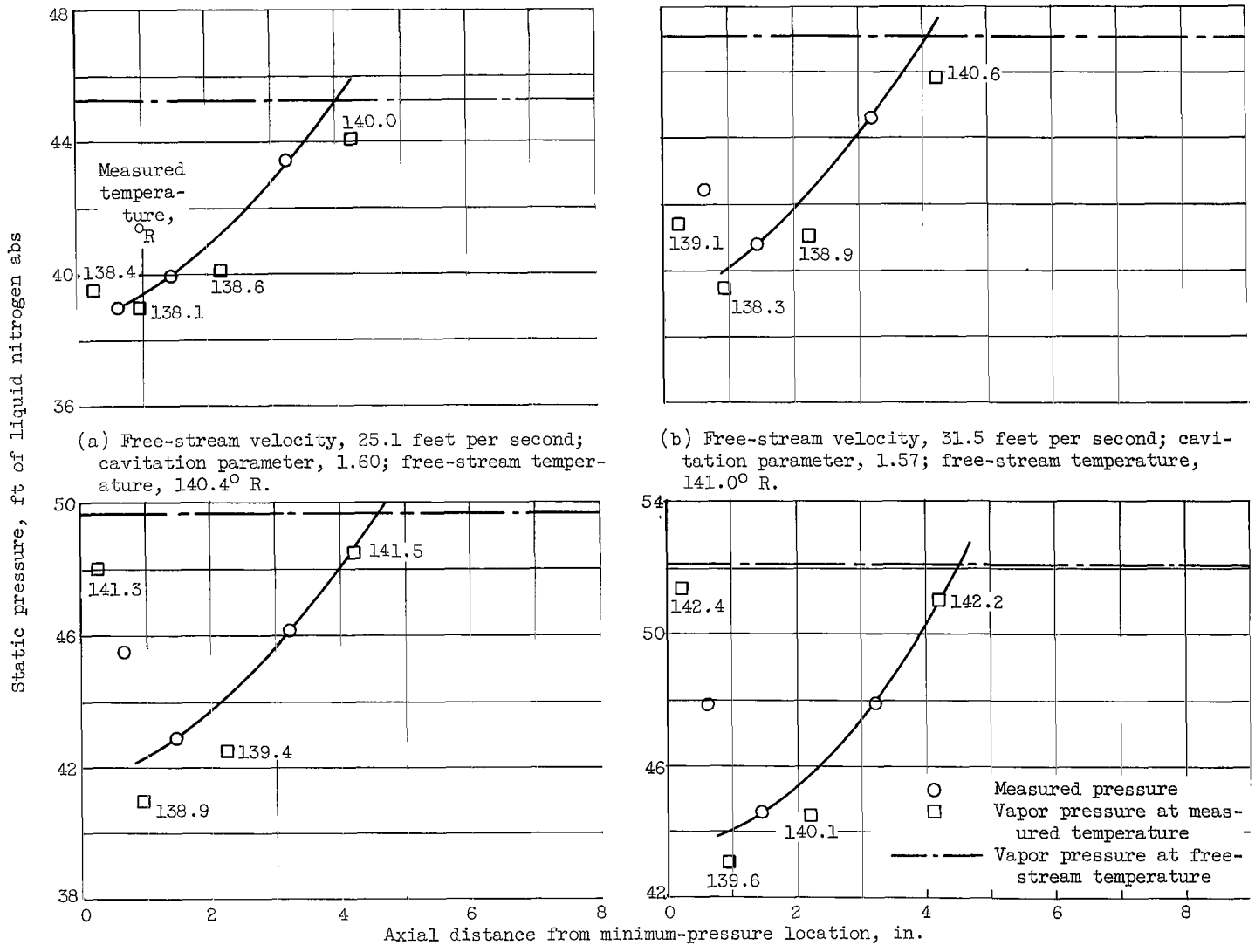

(a) Free-stream velocity, 25.1 feet per second; cavitation parameter, 1.60; free-stream temperature, 140.4° R.

(b) Free-stream velocity, 31.5 feet per second; cavitation parameter, 1.57; free-stream temperature, 141.0° R.

(c) Free-stream velocity, 37.4 feet per second; cavitation parameter, 1.64; free stream temperature, 141.0° R.

(d) Free-stream velocity, 42.0 feet per second; cavitation parameter, 1.68; free-stream temperature, 142.6° R.

Figure 11. - Effect of free-stream velocity on pressure and temperature within nominally fixed extent of nitrogen cavitation ($4\frac{1}{2}$-in. length).

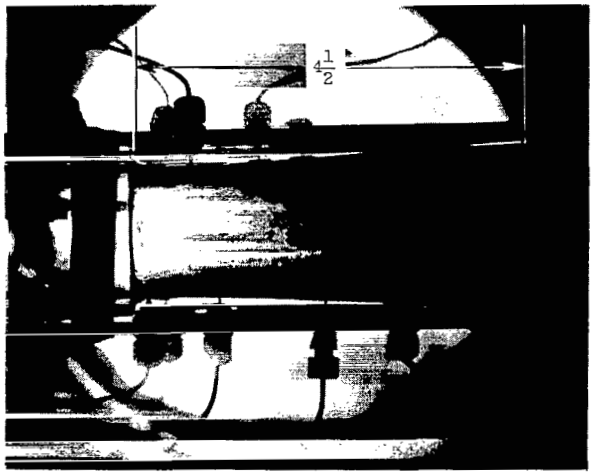

(a) Free-stream velocity, 25.1 feet per second; cavitation parameter, 1.60; free-stream temperature, 140.4° R.

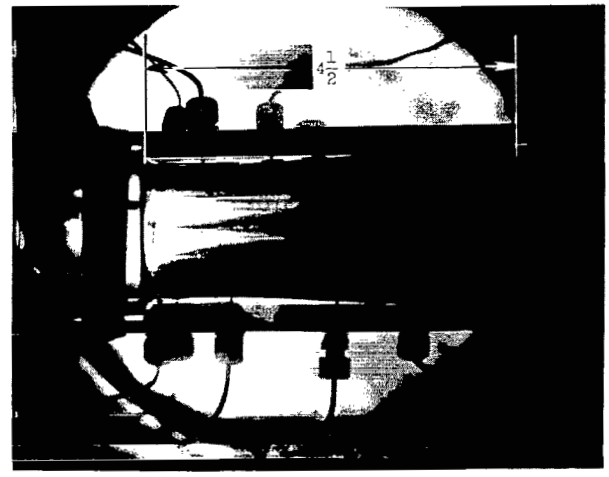

(b) Free-stream velocity, 31.5 feet per second; cavitation parameter, 1.57; free-stream temperature, 141.0° R.

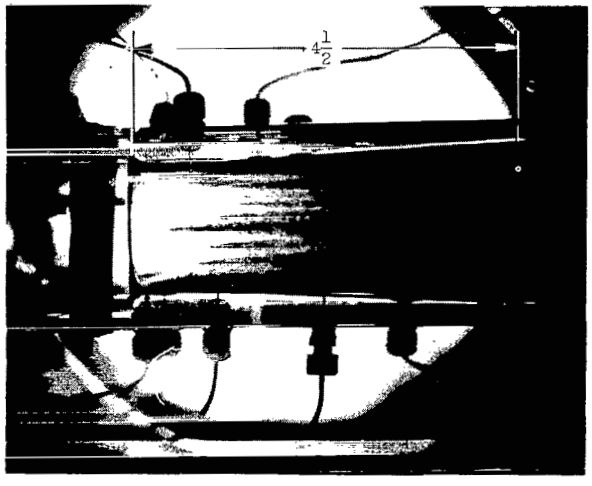

(c) Free-stream velocity, 37.4 feet per second; cavitation parameter, 1.64; free-stream temperature, 141.8° R.

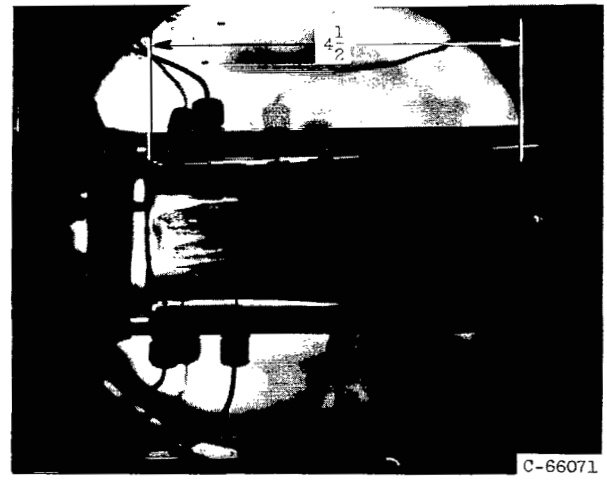

(d) Free-stream velocity, 42.0 feet per second; cavitation parameter, 1.68; free-stream temperature, 142.6° R.

Figure 12. - Effect of free-stream velocity on appearance of nominally fixed extent of nitrogen cavitation ($4\frac{1}{2}$-in. length). Pictures correspond to data in figure 11.

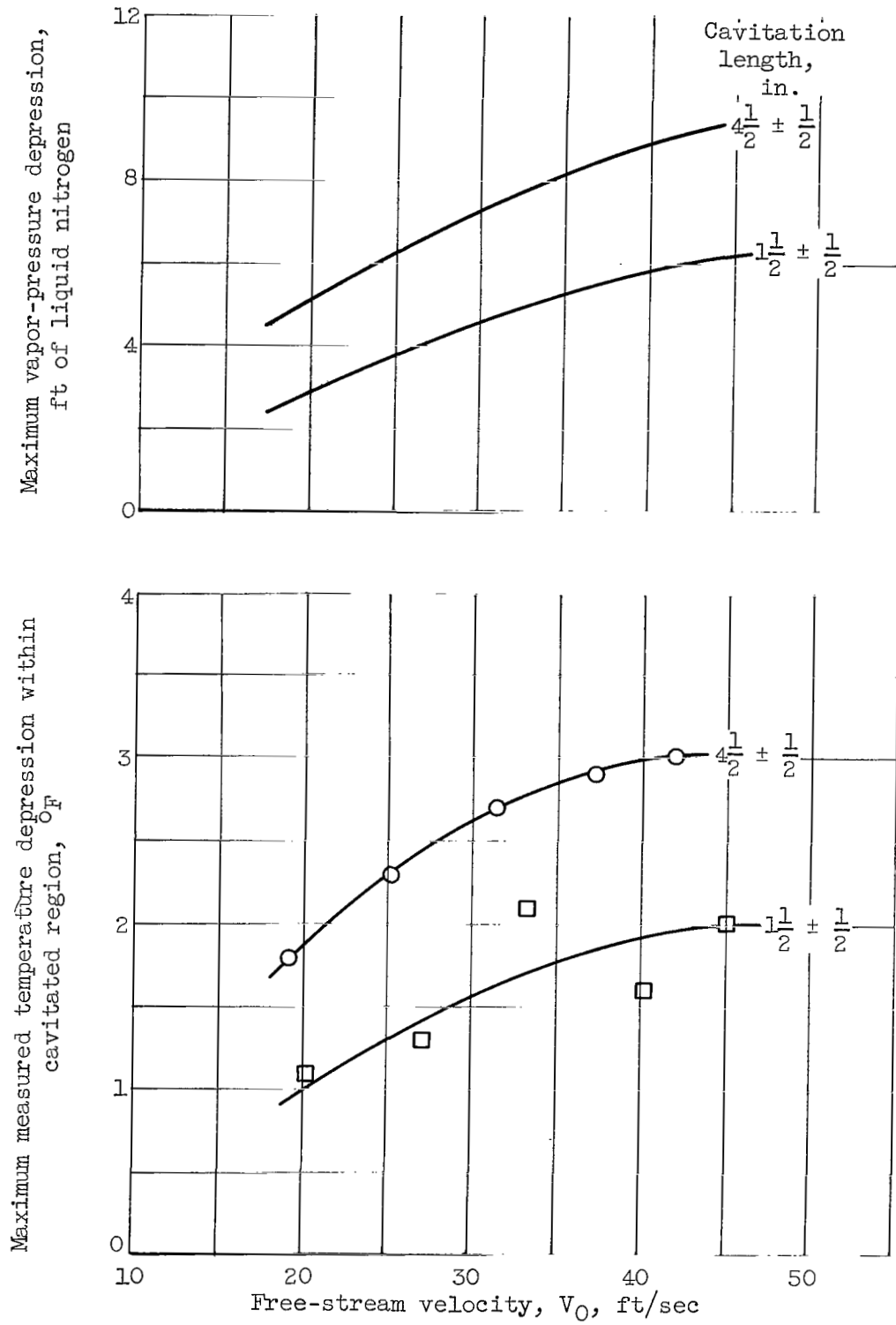

Figure 13. - Effect of free-stream velocity and cavitation length on maximum temperature and vapor-pressure depression within cavitated nitrogen region.

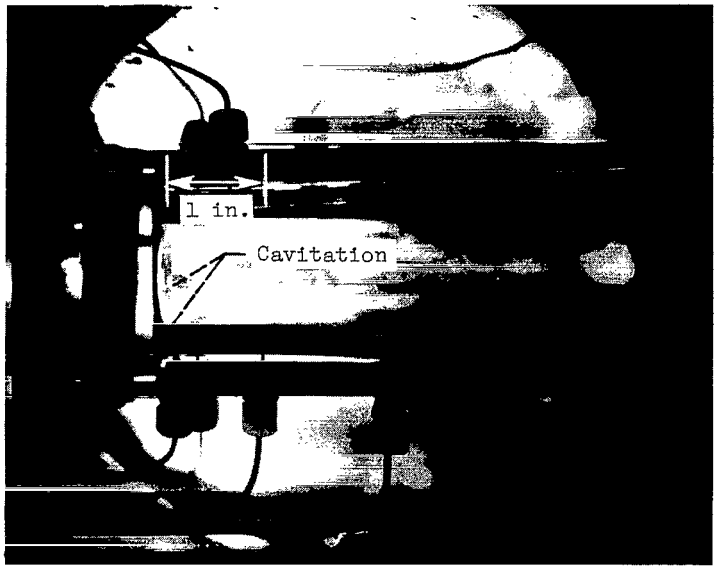

(a) Liquid nitrogen. Free-stream velocity, 46.2 feet per second; cavitation parameter, 2.34; free-stream temperature, 142.7° R.

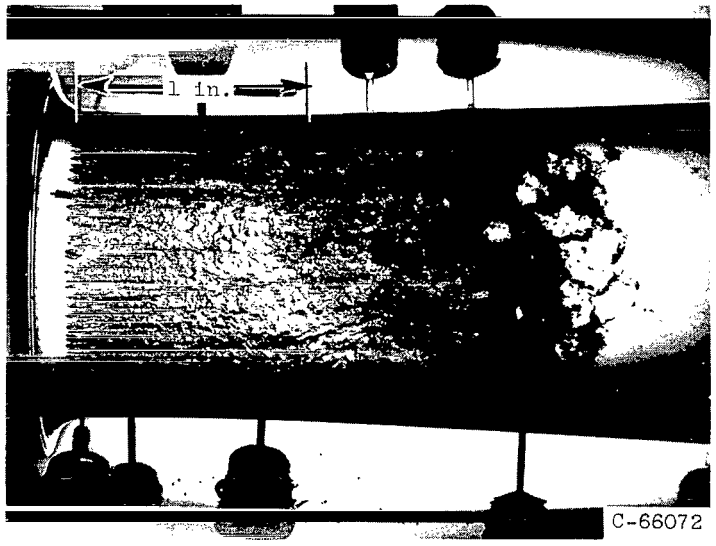

(b) Demineralized water. Free-stream velocity, 37.9 feet per second; cavitation parameter, 2.34; free-stream temperature, 61° F; air content, 9.2 milligrams of air per kilogram of water.

Figure 14. - Comparison of nitrogen and water cavitation for same cavitation parameter and comparable free-stream velocities.